The 19th Conference of Mechanical Engineering Network of Thailand
19-21 October 2005, Phuket, Thailand

A Finite Element Analysis of Natural Convection in an Annulus Induced by Heat Generation within the Inner Solid Cylinder

Worasit Kanjanakijkasem
Department of Mechanical Engineering, Faculty of Engineering, Burapha University
169 Long-Hard Bangsaen Rd., Tambon Saensook, Amphur Maung, Chonburi 20131, Thailand.
E-mail: marveric111@yahoo.com

Abstract

Steady laminar natural convection in an annulus induced by heat generation within the inner solid cylinder has been analyzed by finite element method on standard personal computer. Six-node triangular elements are employed throughout the computational domain. Coincident nodes on the solid-fluid interfaces are utilized to impose the conditions of continuous temperature and heat flux. The annulus with aspect ratio of 0.8 is filled with a Boussinesq fluid with Prandtl number of 0.7. The uniform heat generation rate of the inner solid cylinder is varied to yield the modified Rayleigh number ranging from 3.0×10^3 to 9.0×10^4. The thermal conductivity ratio of 0.1, 1.0, and 10.0 are examined to find the trends of limiting cases. The numerical results show that the surface of the inner cylinder tends to be isothermal and constant-heat-flux when the thermal conductivity ratio approaches infinity and zero, respectively.

Keywords: finite element, natural convection, heat generation, conjugate heat transfer, annulus.

1. Introduction

The phenomenon of natural convection in an enclosure has been intensively researched for several decades because it plays an important role in many engineering applications such as solar energy collector, nuclear reactor designs, cooling of electronic equipment, and thermal storage systems. The enclosures of various shapes have been investigated numerically and experimentally with simplified thermal boundary conditions of constant temperature, constant heat flux, and adiabatic walls [1-5]. But many problems require a more realistic treatment of the thermal wall condition for better designs.

In the recent two decades, many papers concerning to the numerical modeling of conjugate (coupled conduction and convection) heat transfer in enclosures have been published. Kaminski and Prakash [6] considered the effects of conduction in one vertical wall of natural convection in a square enclosure. Lacroix and Joyeux [7] and Dong and Li [8] investigated more complicated problems by including heated cylinder and conducting wall to their computational domains. Liaqat and Baytas [9] simulated the conjugate natural convection in a square enclosure with volumetric sources. These literatures show the increasing of researches on conjugate heat transfer, which reflecting the necessity of realistic simulations for engineering applications.

Natural convection in an annulus between horizontal concentric cylinders has been studied frequently after the research of Kuehn and Goldstein [3] was published. Various aspects of this phenomenon can be found in a number of literatures such as Date [10], Kumar [11], Chung et al. [12], and so on. The condition of higher uniform temperature on the surface of the inner cylinders is preferred. This condition means that the inner cylinder must be heated, which may be induced by heat generation process within it, but the uniformity of the temperature on its surface cannot be guaranteed.

This paper presents the use of finite element method in analyzing the natural convection in an annulus occurring from the mentioned heating process. The conduction within the inner solid cylinder was coupled to the convection within the annular gap and solved simultaneously. The crucial point of the conjugate heat transfer problems is the conditions of continuous temperature and heat flux at the solid-fluid interfaces. In present study, all nodes on the interface were doubled to introduce the auxiliary equations into the system equations to satisfy the conditions at the interface. The method of weighted-residuals was applied in deriving finite element equations based on six-node triangular elements to solve steady-state problems. The corresponding finite element computer program that can be executed on standard personal computer was developed. Flows with modified Rayleigh number ranging from 3.0×10^3 to 9.0×10^4 were simulated. At each modified Rayleigh number, the thermal conductivity ratio of 0.1, 1.0, and 10.0 were examined to pursue the uniform temperature on the inner cylinder surface and investigate the heat transfer characteristics of the flows. Some results could be indirectly compared with the numerical solutions of Kuehn and Goldstien [3] to verify the developed finite element computer program.

2. Governing Equations

Following assumptions are made to simplify the problems: there is no viscous dissipation, the fluid properties are constant at reference temperature, the Boussinesq approximation is taken into account for fluid density variation due to buoyancy, and the radiation heat exchange and thermal expansion effect are neglected. If the gravitational force acts in the vertical direction, the governing equations for two-dimensional steady laminar incompressible flows of a Newtonian fluid can be written in the following form [13,14]: -

Conservation of Mass:

$$\frac{\partial u}{\partial x}+\frac{\partial v}{\partial y}=0 \tag{1}$$

Conservation of *X*-Momentum:

$$\rho_f\left(u\frac{\partial u}{\partial x}+v\frac{\partial u}{\partial y}\right)=\frac{\partial \sigma_x}{\partial x}+\frac{\partial \tau_{yx}}{\partial y} \tag{2}$$

Conservation of *Y*-Momentum:

$$\rho_f\left(u\frac{\partial v}{\partial x}+v\frac{\partial v}{\partial y}\right)=\frac{\partial \tau_{xy}}{\partial x}+\frac{\partial \sigma_y}{\partial y} -\rho_f g\left[1-\beta_f(T_f-T_{ref})\right] \tag{3}$$

Conservation of Energy:

$$\rho_f c_{pf}\left(u\frac{\partial T_f}{\partial x}+v\frac{\partial T_f}{\partial y}\right)=q_f'''-\frac{\partial q_x}{\partial x}-\frac{\partial q_y}{\partial y} \tag{4}$$

where x and y are Cartesian coordinates, u and v are the velocity component in x- and y-direction, T_f is the fluid temperature, ρ_f is the fluid density, β_f is the fluid thermal expansion coefficient, c_{pf} is the specific heat at constant pressure of fluid, q_f''' is the rate of volumetric heat generation of fluid, T_{ref} is the fluid reference temperature, and g is the gravitational acceleration.

The fluid reference temperature for the buoyant term in y-momentum equation is the average temperature of fluid [15]. The arithmetic mean of the maximum and minimum fluid temperature is used as the fluid reference temperature throughout this paper because the fluid temperature variations are small.

The stress components are given by

$$\sigma_x=-p+2\mu\frac{\partial u}{\partial x} \tag{5}$$

$$\sigma_y=-p+2\mu\frac{\partial v}{\partial y} \tag{6}$$

$$\tau_{yx}=\tau_{xy}=\mu\left(\frac{\partial u}{\partial y}+\frac{\partial v}{\partial x}\right) \tag{7}$$

where p is the fluid pressure and μ is the fluid dynamic viscosity.

From Fourier's law of conduction for isotropic materials, heat flux in x- and y-direction are

$$q_x=-k_f\frac{\partial T_f}{\partial x},\ q_y=-k_f\frac{\partial T_f}{\partial y} \tag{8}$$

where k_f is the fluid thermal conductivity.

For a conducting solid at steady state, the energy equation is

$$0=q_s'''-\frac{\partial q_x}{\partial x}-\frac{\partial q_y}{\partial y} \tag{9}$$

where q_s''' is the rate of heat generation per unit volume of solid.

Heat flux in x- and y-direction are

$$q_x=-k_s\frac{\partial T_s}{\partial x},\ q_y=-k_s\frac{\partial T_s}{\partial y} \tag{10}$$

where k_s is the solid thermal conductivity.

For steady laminar natural convection in enclosures, temperature must be specified at least one point on the no-slip walls. On the other portions of the wall, temperatures or heat fluxes are described. When the conjugate effects are considered, the temperatures and heat fluxes must be continuous at the solid-fluid interfaces and the remaining boundary of the conducting solid may be described by temperatures or heat fluxes.

3. Finite Element Formulation

Yamada et al. [16] suggested the use of different order interpolation functions to avoid the over-constrained system of algebraic equations. So, the six-node triangular elements are utilized in deriving finite element equations because they offer the choice for different order interpolation functions [17]. The interpolation functions of all unknowns in six-node triangular elements are: -

Second Order Interpolation Functions for Velocity Components and Temperature:

$$\begin{aligned} N_1&=L_1^2-L_1(L_2+L_3) \qquad & N_4&=4L_2L_3\\ N_2&=L_2^2-L_2(L_3+L_1) \qquad & N_5&=4L_3L_1\\ N_3&=L_3^2-L_3(L_1+L_2) \qquad & N_6&=4L_1L_2 \end{aligned} \tag{11}$$

First Order Interpolation Functions for Pressure:

$$H_1=L_1 \qquad H_2=L_2 \qquad H_3=L_3 \tag{12}$$

where L_1, L_2, L_3 are shape functions of triangle.

The method of weighted-residuals was applied by weighting the conservation of momentum and energy with second order interpolation functions and the conservation of mass with first order interpolation functions. This procedure yields 21 equations for determining 21 unknowns on each element. After applying integration by-parts and Gauss theorem, the finite element equations are: -

For fluid elements,

$$\int_{\Omega_e}\left[N_\alpha\rho_f(uu_{,x}+vu_{,y})+(N_{\alpha,x}\sigma_x+N_{\alpha,y}\tau_{yx})\right]d\Omega_e =\int_{\Gamma_e}N_\alpha P_x d\Gamma_e \tag{13}$$

$$\int_{\Omega_e}\left[N_\alpha\rho_f(uv_{,x}+vv_{,y})+(N_{\alpha,x}\tau_{xy}+N_{\alpha,y}\sigma_y)\right]d\Omega_e +\int_{\Omega_e}N_\alpha\rho_f g\left[1-\beta_f(T_f-T_{ref})\right]d\Omega_e =\int_{\Gamma_e}N_\alpha P_y d\Gamma_e \tag{14}$$

$$\int_{\Omega_e}\left[N_\alpha\rho_f c_{p_f}(uT_{f,x}+vT_{f,y})-N_{\alpha,x}q_x-N_{\alpha,y}q_y\right]d\Omega_e =\int_{\Omega_e}N_\alpha q_f''' d\Omega_e-\int_{\Gamma_e}N_\alpha(q_n)_f\,d\Gamma_e \tag{15}$$

$$\int_{\Omega_e} H_\lambda (u_{,x} + v_{,y}) d\Omega_e = 0 \qquad (16)$$

where Ω_e is the area of fluid element, Γ_e is the boundary of fluid element, $\lambda = 1, 2, 3$, and $\alpha = 1, 2, ..., 6$.

The components of surface forces are defined by

$$P_x = \sigma_x l + \tau_{yx} m \qquad (17)$$

$$P_y = \tau_{xy} l + \sigma_y m \qquad (18)$$

and the rate of heat transfer in the outward normal direction of fluid element is defined by

$$(q_n)_f = q_x l + q_y m \qquad (19)$$

where l and m are direction cosines of the outward normal vector of the fluid element boundary.
For solid elements,

$$-\int_{\Omega_e} (N_{\alpha,x} q_x + N_{\alpha,y} q_y) d\Omega_e = \int_{\Omega_e} N_\alpha q_s''' d\Omega_e - \int_{\Gamma_e} N_\alpha (q_n)_s d\Gamma_e \qquad (20)$$

where Ω_e is the area of solid element, Γ_e is the boundary of solid element, and $\alpha = 1, 2, ..., 6$.

The rate of heat transfer in the outward normal direction of solid element is defined by

$$(q_n)_s = q_x l + q_y m \qquad (21)$$

where l and m are direction cosines of the outward normal vector of the solid element boundary.

After substituting the constitutive equations of stress components and heat fluxes into equations (13) to (16) and equation (20), the finite element equations become

$$\left[K_f\right]_e \left\{\phi_f\right\}_e = \left\{Q_f\right\}_e \qquad (22)$$

$$\left[K_s\right]_e \left\{\phi_s\right\}_e = \left\{Q_s\right\}_e \qquad (23)$$

where $[K_f]_e$ and $[K_s]_e$ are element property matrices (stiffness matrices) of fluid and solid media, $\{\phi_f\}_e$ is the vector of fluid element unknowns (velocity components, temperature, and pressure), and $\{\phi_s\}_e$ is the vector of solid element unknowns (temperature).

$\{Q_f\}_e$ and $\{Q_s\}_e$ are the vectors of physical boundary conditions (load vectors) on the fluid elements boundary and solid elements boundary, respectively.

After assembling all elements together, the system equations are

$$\left[K\right]_{sys} \left\{\phi\right\}_{sys} = \left\{Q\right\}_{sys} \qquad (24)$$

where $[K]_{sys}$ is system property matrix, $\{\phi\}_{sys}$ is the system vector of unknowns, and $\{Q\}_{sys}$ is the system vector of physical boundary conditions on the domain boundary.

All of the boundary conditions including the special conditions at the solid-fluid interface must be imposed before solving the system equations. The continuity of temperature and heat flux at solid-fluid interface are satisfied by modifying two energy equations at the coincident nodes (one equation for solid media and the another one for fluid media) as follow.

$$T_f - T_s = 0 \qquad (25)$$

$$(q_n)_f + (q_n)_s = 0 \qquad (26)$$

The latter equation is accomplished by summing the left-hand side of the energy equations of the coincident nodes.

4. Computational Procedures

Because the system equations are nonlinear, Newton-Raphson iterative method is applied to change them into a system of linear equations of unknown increments.

$$\left[\partial K / \partial \phi\right]_{sys} \left\{\Delta\phi\right\}_{sys} = \left\{R\right\}_{sys} \qquad (27)$$

where $\{\Delta\phi\}_{sys}$ is the vector of unknown increments and $\{R\}_{sys}$ is the vector of residuals.

The Newton-Raphson iterative process is terminated when 1-norm [18] relative error (ε) is less than 0.1%. The preconditioning conjugate gradient method [19] is applied in solving equation (27) with the stopping criteria of 10^{-6} in 2-norm [18] relative residuals.

$$\varepsilon = \frac{\sum_{i=1}^{n} \left|(\Delta\phi_i)\right|}{\sum_{i=1}^{n} \left|(\phi_i)\right|} \times 100\% \qquad (28)$$

The final form of the system equations of unknown increments is used in the development of the finite element computer program that can be executed on standard personal computers. The developed computer program is verified by examining the trends of limiting cases with the results of Kuehn and Goldstien [3]. Some numerical results that cannot be compared are generated for investigating other information of this phenomenon.

5. Numerical Results and Discussion

Figure 1 shows the physical situation and finite element mesh to be analyzed. The outer cylinder with diameter d_o is cylindrical shell with negligible thickness and is fixed at low temperature. The inner solid cylinder with diameter d_i generates volumetric heat at the rate of q_s''' uniformly over its cross section and has constant properties. These two cylinders form an annulus with a width of w. This annular gap is filled with a Newtonian fluid with constant properties that cannot supply any volumetric heat generation (q_f'''=0).

Only a half of the physical domain is considered because many former researches indicate the symmetry of the solutions of this problem. The finite element model consists of 8386 nodes of velocities and temperature, 2167 nodes of pressure, and 4054 elements is employed in all simulations of this paper.

The influenced parameters of the natural convection in an annulus with constant temperature surfaces are Prandtl number (Pr), Rayleigh number (Ra), and the ratio of annular gap width to the inner cylinder diameter (w/d_i). Prandtl number and Rayleigh number are defined by

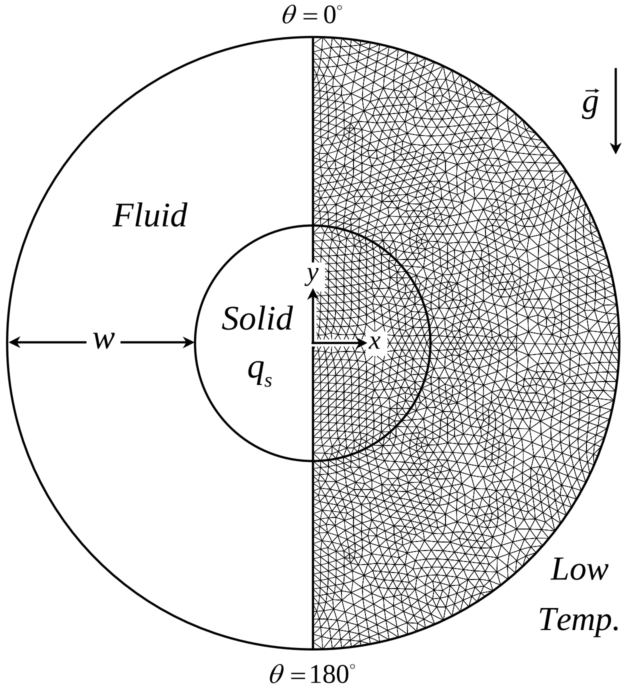

Figure 1. Physical situation and finite element model.

$$Pr = \frac{\nu}{\kappa_f} = \frac{\mu c_{pf}}{k_f} \tag{29}$$

$$Ra = \frac{g\beta_f \left(T_{\max} - T_{\min}\right) l_f^3}{\nu\kappa_f} \tag{30}$$

where ν is the fluid kinematic viscosity, κ_f is the fluid thermal diffusivity, and l_f is the characteristic length of fluid domain. For this geometry, the annular gap width (w) acts as the characteristic length.

When the natural convection is induced by heat generation of the inner solid cylinder, the problem is said to be conjugate. A new influenced parameter, the thermal conductivity ratio must be introduced.

$$K = k_s / k_f \tag{31}$$

Rayleigh number must be modified by the equation

$$Ra^* = \frac{g\beta_f l_f^3}{\nu\kappa_f} \cdot \frac{q_s''' l_s^2}{k_f} \tag{32}$$

where l_s is the characteristic length of solid domain. Now, the diameter of the inner solid cylinder (d_i) acts as the characteristic length of solid domain.

The new factor in equation (32) indicates the strength of volumetric heat generation of the inner cylinder. It has the dimension of temperature and is the cause of fluid motion like the factor ($T_{\max}$-$T_{\min}$) in equation (30). The fluid thermal conductivity is selected instead that of solid because the natural convection characterized by this parameter occur in the fluid media.

In present study, the fluid filled in the annulus has Prandtl number of 0.7 (air) and the aspect ratio, the ratio of annular gap width to the inner cylinder diameter, is 0.8 for all cases. The conductivity ratio of 0.1, 1.0, and 10.0 are examined to find the trends of the limiting cases when it approaches zero and infinity at the modified Rayleigh number of 3.0×10^3, 6.0×10^3, 1.0×10^4, 2.0×10^4, 3.6×10^4, and 9.0×10^4. All of numerical solutions presented here are obtained by executing the finite element computer program on Pentium III 866 MHz with 256-MB memory on board.

The velocity distributions are not shown here because the most interested point of this paper is the thermal effect of heat generating process from the inner solid cylinder on the temperature distributions and heat transfer performances.

The non-dimensional temperature in all figures is defined based on the difference of maximum and minimum temperatures overall the domain by

$$\Theta = \frac{T - T_{\min}}{T_{\max} - T_{\min}} \tag{33}$$

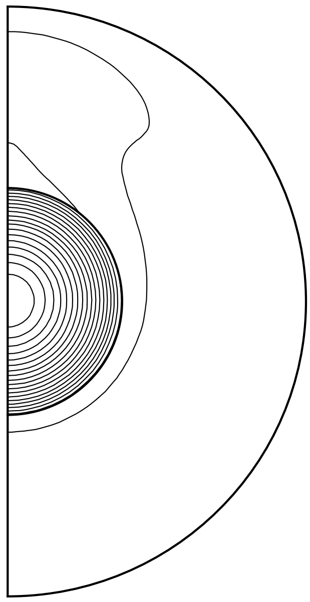

(a) K=0.1

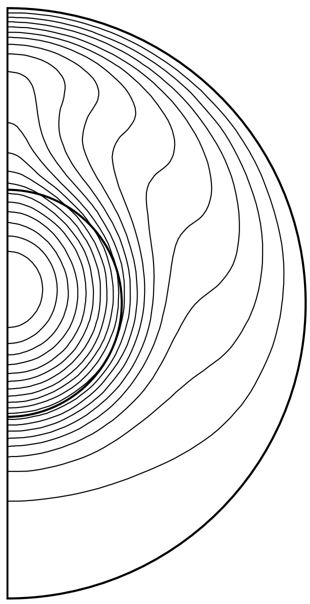

(b) K=1.0

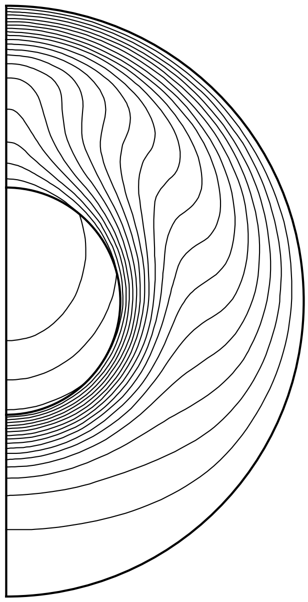

(c) K=10.0

Figure 2. Temperature distributions at $Ra^* = 9.0\times10^4$.

The temperature distribution at the highest modified Rayleigh number is presented in Figure 2. Twenty-level isotherm from Θ=0 to Θ=0.95 are employed without labeling to keep the clarity of the temperature distributions. The position of highest temperature in the computational domain (Θ=1.0) is not shown by the same reason. The distorted isotherms in Figure 2 indicate that the thermal energy generated from the inner cylinder predominantly transfers to the outer cylinder by convection. More distortion of isotherms is expected at higher modified Rayleigh number.

It can be seen from Figure 2 that most of the isotherms are densely compressed within the inner solid cylinder when K=0.1 and are expanded into the fluid-filled annular gap when K increases. This means that the temperature gradient within the inner solid cylinder is high when it behaves as an insulator (K is lower than 1.0) to give the conduction rate within the solid cylinder identical to the convection rate in the annular gap, or vice versa.

The abrupt changes in curvature of isotherms in Figure 2 when conductivity ratio is different from unity are emphasized again in Figure 3 by the abrupt changes in the gradients of non-dimensional radial temperature distributions at the solid-fluid interface of three angular positions.

The temperature distributions on the solid-fluid interface at the same modified Rayleigh number are presented in Figure 4. They display the influence of K on the non-dimensional temperatures on the interfaces. The lower values of non-dimensional temperatures do not mean that the dimensional temperatures do because the maximum temperatures increase when K is decreased.

From the numerical results, it can be inferred that the surface of the inner cylinder tends to be isothermal when K approaches infinity. The Rayleigh number defined in equation (30) must be calculated at each modified Rayleigh number to compare with the results of Kuehn and Goldstein [3].

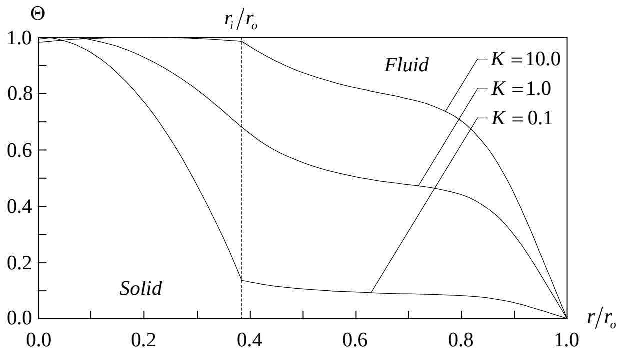

(a) θ=0°

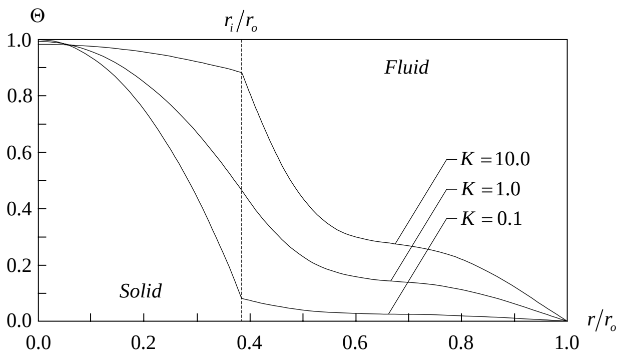

(b) θ=90°

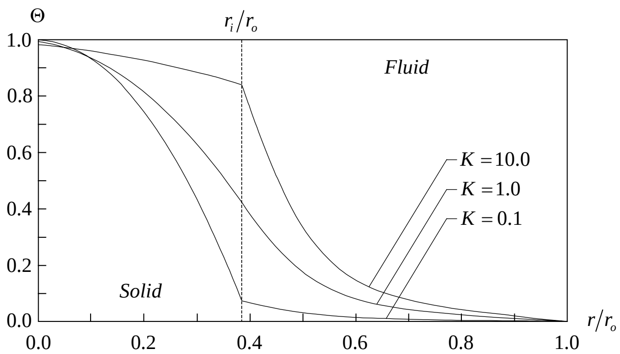

(c) θ=180°

Figure 3. Radial temperature distributions at $Ra^* = 9.0\times10^4$.

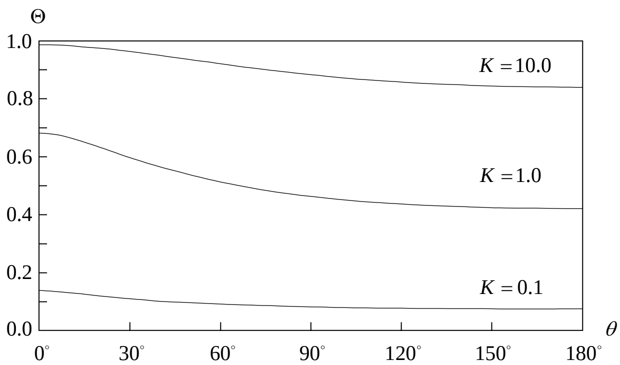

Figure 4. Temperature distributions on solid-fluid interface at $Ra^* = 9.0\times10^4$.

The corresponding Rayleigh numbers calculated from equation (30) by using the average temperatures of the inner cylinder surface when K=10.0 as $T_{\max}$ are in Table 1. The cases with modified Rayleigh number of 3.6×10^4 and 9.0×10^4 give Rayleigh numbers that can be closely matched with the cases when Rayleigh numbers are 3,000 and 6,000 of Kuehn and Goldstein [3]. For brevity of representation, only the latter case comparison is explained.

Table 1 Corresponding Rayleigh numbers when K=10.0.

Ra^*	Ra
3.0×10^3	348
6.0×10^3	675
1.0×10^4	1,068
2.0×10^4	1,890
3.6×10^4	2,955
9.0×10^4	5,939

The numerical values in Table 1 may be slightly changed if the different sets of numerical properties, which give the same Prandtl number and modified Rayleigh number, are employed. But the set of numerical properties that results in small temperature difference on the inner cylinder surface is recommended.

The equivalent thermal conductivity ratios are calculated for quantitative comparisons. They are the ratios between heat transfer by convection and pure conduction (no fluid motion) defined by the following equations.

For Heat Gain from the Inner Cylinder Surface:

$$\frac{k_{eq}}{k_f} = \frac{\left(\dfrac{\partial T_f}{\partial x} l + \dfrac{\partial T_f}{\partial y} m\right)}{\dfrac{T_{\max} - T_{\min}}{r_i \ln(r_o/r_i)}} \tag{34}$$

For Heat Loss from the Outer Cylinder Surface:

$$\frac{k_{eq}}{k_f} = -\frac{\left(\dfrac{\partial T_f}{\partial x} l + \dfrac{\partial T_f}{\partial y} m\right)}{\dfrac{T_{\max} - T_{\min}}{r_o \ln(r_o/r_i)}} \tag{35}$$

where r_i and r_o are the inner and outer cylinder radius, and k_{eq} is the equivalent thermal conductivity.

The maximum temperatures in equation (34) and (35) are the average temperatures of the inner cylinder surface when K=10.0 used in equation (30) as mentioned above. While the minimum temperature is the outer cylinder surface.

Figure 5 and Figure 6 show the trends of equivalent thermal conductivity ratios on the inner and outer cylinder surfaces when K approaches to zero and infinity. On the inner cylinder surface, the series of curves in Figure 5 indicates that the curve tends to be identical to the isothermal surface when K is greater than unity. On the other hand, the decreasing in K lower than unity flattens the curve to be the constant-heat-flux surface. So the curves in Figure 6 present the equivalent thermal conductivity ratios of the outer cylinder when the inner cylinder surface approaches to be the isothermal and constant-heat-flux surfaces.

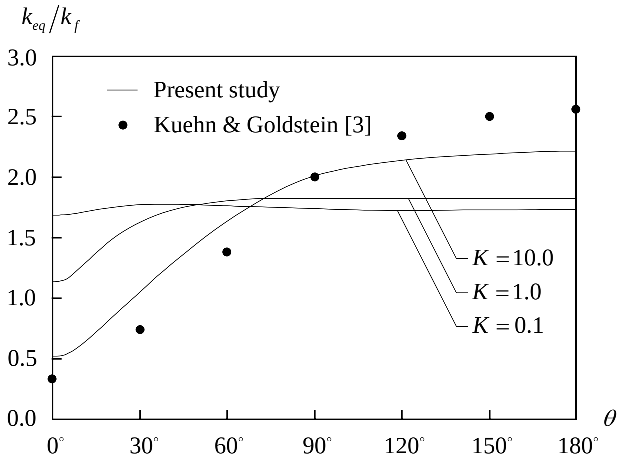

Figure 5. Local equivalent thermal conductivity ratios on the inner cylinder surface at $Ra^* = 9.0\times10^4$.

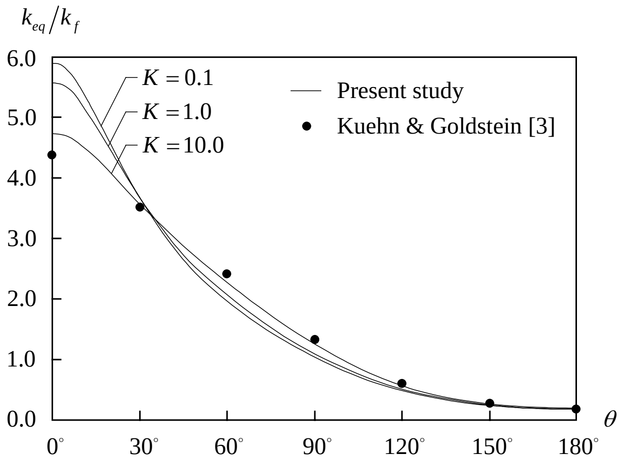

Figure 6. Local equivalent thermal conductivity ratios on the outer cylinder surface at $Ra^* = 9.0\times10^4$.

The average values of the equivalent thermal conductivity ratios based on the average temperatures of the inner cylinder surface when K=10.0 at each modified Rayleigh numbers are summarized in Table 2. The agreements between the numerical values of the last two cases in Table 2 and that of Kuehn and Goldstein [3] confirm the validity of other values and verify the reliability of the developed finite element computer program.

Finally, the discrepancy within 1% of the average equivalent conductivity ratios at each modified Rayleigh number in Table 2 guarantees the existence of the set of the influenced parameters that characterizes the conjugate natural convection under this situation. The set of influenced parameters consists of Prandtl number (Pr), modified Rayleigh number (Ra^*), the ratio of annular gap width to the inner cylinder diameter (w/d_i), and the thermal conductivity ratio (K).

Table 2 Average equivalent thermal conductivity ratios on cylinder surfaces.

Ra^*	Surface Location	K		
		0.1	1.0	10.0
3.0×10^3	Inner	1.012	1.010	1.008
	Outer	1.013	1.013	1.013
6.0×10^3	Inner	1.043	1.041	1.038
	Outer	1.044	1.044	1.044
1.0×10^4	Inner	1.099	1.097	1.094
	Outer	1.099	1.099	1.099
2.0×10^4	Inner	1.242	1.240	1.236
	Outer	1.242	1.242	1.242
3.6×10^4	Inner	1.409	1.408	1.404
	Outer	1.414	1.414	1.412
9.0×10^4	Inner	1.731	1.731	1.725
	Outer	1.742	1.740	1.734

6. Conclusion

Finite element analysis for steady laminar natural convection in an annulus induced by heat generation within the inner solid cylinder has been performed. The complete set of influenced parameters of this problem was defined. When the thermal conductivity ratio is very large, the inner cylinder surface tends to be isothermal surface. The constant-heat-flux inner cylinder surface may be attained when the thermal conductivity ratio is very low. Some numerical results that can be compared with the results of the classical research concerning to the natural convection in horizontal annulus show very good agreements in overall heat transfer performance. This consistency confirms the reliability of the developed computer program.

The concept of this paper can be extended to solve other multi-physics problems by doubling the nodes on the interfaces. A number of equations are introduced into the system equations for preserving the continuity of essential and physical boundary conditions (temperature and heat flux in present study) across the interfaces. This increases the complexities of the problems and requires more CPU time to solve, but the numerical results for superior designs are available.

Acknowledgment

This research was financially supported by the Faculty of Engineering, Burapha University, contract no. 27/2548.

References

[1] C.D. Upson, P.M. Gresho, and R.L. Lee, "Finite Element Simulations of Thermally Induced Convection in an Enclosed Cavity", Lawrence Livermore Laboratory, University of California (Informal Report), 1980.

[2] G.D. Vahl Davis, "Natural Convection of Air in a Square Cavity: a bench mark numerical solution", Int. J. Numerical Methods in Fluids, Vol. 3, 1983, pp. 249-264.

[3] T.H. Kuehn, and R.J. Goldstein, "An Experimental and Theoretical Study of Natural Convection in the Annulus between Horizontal Concentric Cylinders", J. Fluid Mechanics, No. 74, 1976, pp. 695-719.

[4] M.M. Ganzarolli, and L.F. Milanez, "Natural Convection in Rectangular Enclosures Heated from below and Symmetrically Cooled from the Sides", Int. J. Heat Mass Transfer, Vol. 38, 1995, pp. 1063-1073.

[5] C.J. Ho, W.S. Chang, and C.C. Wang, "Natural Convection between Two Horizontal Cylinders in an Adiabatic Circular Enclosure", J. Heat Transfer, Vol. 115, 1993, pp. 158-165.

[6] D.A. Kaminski, and C. Prakash, "Conjugate Natural Convection in a Square Enclosure Effect of Conduction in One of the Vertical Walls", Int. J. Heat Mass Transfer, Vol. 29, 1986, pp. 1979-1988.

[7] M. Lacroix, and A. Joyeux, "Coupling of Wall Conduction with Natural Convection from Heated Cylinders in a Rectangular Enclosure", Int. Commun. Heat Mass Transfer, Vol. 23, 1996, pp. 143-151.

[8] S.-F. Dong, and Y.-T. Li, "Conjugate of Natural Convection and Conduction in a Complicated Enclosure", Int. J. Heat Mass Transfer, Vol. 47, 2004, pp. 2233-2239.

[9] A. Liaqat, and A.C. Baytas, "Conjugate Natural Convection in a Square Enclosure Containing Volumetric Sources", Int. J. Heat Mass Transfer, Vol. 44, 2001, pp. 3237-3280.

[10] A.W. Date, "Numerical Prediction of Natural Convection Heat Transfer in Horizontal Annulus", Int. J. Heat Mass Transfer, Vol. 29, 1986, pp. 1457-1467.

[11] R. Kumar, "Study of Natural Convection in Horizontal Annuli", J. Heat Mass Transfer, Vol. 31, 1988, pp. 1147-1158.

[12] J.D. Chung, C.-J. Kim, H. Yoo, and J.S. Lee, "Numerical Investigation on the Bifurcative Natural Convection in a Horizontal Concentric Annulus", Numerical Heat Transfer Part A: Applications, Vol. 36, No. 3, 1999, pp. 291-307.

[13] H. Schlichting, Boundary-Layer Theory, McGraw-Hill, New York, 1979.

[14] P.K. Kundu, and I.M. Cohen, Fluid Mechanics, Academic Press, New York, 2002.

[15] F.S. Sherman, Viscous Flow, McGraw-Hill, Singapore, 1990.

[16] Y. Yamada, K. Ito, Y. Yokouchi, T. Tamano, and T. Ohtsubo, "Finite Element Analysis of Steady Fluid and Metal Flow", Finite Elements in Fluids, Vol. 1, John Wiley & Sons, New York, 1975, pp. 73-94.

[17] K.H. Huebner, and E.A. Thornton, The Finite Element Method for Engineers, John Wiley & Sons, New York, 1982.

[18] R.J. LeVeque, Finite Difference Methods for Differential Equations, Lecture note in course AMATH 585-6, University of Washington, 1998.

[19] W.H. Press, S.A. Teukolsky, W.T. Vettering, and B.P. Flannery, Numerical Recipes in FORTRAN 77, Cambridge University Press, U.K., 1992.